Targeted disruption of H3 receptors results in changes in brain histamine tone leading to an obese phenotype

Kazuhiko Takahashi, Hiroaki Suwa, Tomoo Ishikawa, and Hidehito Kotani

Functional Genomics, Banyu Tsukuba Research Institute in collaboration with Merck Research Laboratories, Tsukuba, Ibaraki, Japan

Histamine is an aminergic neurotransmitter that is localized in the CNS and in peripheral tissues. To date, four histamine receptors have been identified, and the H3 receptor, which was recently cloned, is predominantly expressed in the CNS. The peripheral functions of histamine have been investigated intensively using available molecular and pharmacological tools, and the molecular identification of the H3 receptor opens up new possibilities for investigating the role of histamine in central tissues. To understand the biological function of the histamine presynaptic autoreceptor H3, we inactivated the receptor through homologous recombination. $H3^{-/-}$ mice manifest mild obese phenotypes that are characterized by increases in body weight, food intake, and adiposity and by reductions in energy expenditure. Consistent with these observations, homozygous null mice have insulin and leptin resistance, increased levels of plasma leptin and insulin, and decreased levels of histamine in the hypothalamic/thalamic region of their brains coupled with increased histamine turnover. The expression of *UCP1* in brown adipose tissue and of *UCP3* in brown adipose tissue, white adipose tissue, and skeletal muscle is decreased in $H3^{-/-}$ mutants, and the anorexigenic activity of thioperamide is not observed. These results suggest that neuronal histamine is a mediator of body-weight homeostasis and that neuronal histamine functions through H3 receptors in mice.

J. Clin. Invest. **110**:1791–1799 (2002). doi:10.1172/JCI200215784.

Introduction

Histamine is a potent bioactive substance that has been studied for nearly a century. Histamine is stored in the mast cells of peripheral tissues, and histamine release has been implicated in the pathogenesis of various inflammatory reactions (1–3). Also, histamine is an aminergic neurotransmitter that is localized in the CNS and the peripheral nervous system. Histaminergic neurons are located exclusively in the tuberomammillary nucleus (TM) of the posterior hypothalamus and project their axons into brain regions including the hypothalamus, thalamus, cerebral cortex, amygdala, and septum (4–7).

There are four histamine receptors that have been identified: H1, H2, H3, and H4 (4, 8–10). In general, histamine has been shown to modulate inflammatory responses through H1 receptors and to modulate gastric acid secretion through H2 receptors. This led to the discovery and therapeutic use of potent H1 and H2 receptor antagonists. In contrast to H1, H2, and H4 receptors, H3 receptors are predominantly expressed in the CNS (9, 10), act as autoreceptors in presynaptic neurons, and control histamine turnover. H3 receptors have also been shown to act as heteroreceptors in dopamine-, serotonin-, noradrenaline- , GABA-, and acetylcholine-containing neurons (11). Since H3 receptors are located predominantly in the CNS, it has been suggested that H3 receptors mediate various CNS functions by modulating brain histaminergic tone and possibly by collaborating with H1 and H2 receptors. Histamine has been implicated in the regulation of arousal state (12), locomotor activity (13), cardiovascular control (14), water intake (15), food intake (16), and memory formation (17). In fact, H1 knockout mice have been shown to have circadian rhythms and locomotor activities that are disturbed and exploratory behavior that is impaired. This suggests that H1 receptors are important in some histamine functions (18). However, the functions of H3 receptors with respect to the pharmacological effects of histamine in the CNS are not clear.

A number of studies have indicated that histamine may suppress appetite and the hypothalamic histaminergic neurons that participate in the regulation of food intake (19–21). Histamine that is injected intracerebroventricularly is a potent appetite suppressant, and depletion of histamine stimulates feeding (22). Changes in histaminergic tone in the CNS have been associated with genetic models of obesity (23). In addition, intracerebroventricular injection of leptin has been correlated with changes in the turnover rate of

Received for publication April 24, 2002, and accepted in revised form November 6, 2002.

Address correspondence to: Hidehito Kotani, Banyu Tsukuba Research Institute, Okubu 3, Tsukuba, Ibaraki, 300-2611, Japan. Phone: 298-77-2202; Fax: 298-77-2027; E-mail: kotanihh@banyu.co.jp.

Conflict of interest: The authors have declared that no conflict of interest exists.

Nonstandard abbreviations used: tuberomammillary nucleus (TM); ventromedial nucleus (VMH); arcuate nucleus (ARH); embryonic stem (ES); neomycin (neo); N-α-methylhistamine (NAMHA); degradation per minute (dpm); brown adipose tissue (BAT); white adipose tissue (WAT); triacyl glycerol (TG); neuropeptide Y (NPY); histamine N-methyltransferase (HMT); melanin-concentrating hormone (MCH).

hypothalamic neuronal histamine (24). In both humans and rodents, treatment with an H1 antagonist resulted in hyperphagia (25), and administration of H3 antagonists led to hypophagia (26–30). H1 and H3 receptor mRNA was detected in the ventromedial nucleus (VMH) and the arcuate nucleus (ARH) of the hypothalamus (9). These data suggest that the modulation of hypothalamic histamine by H3 receptors, possibly by signaling through H1 receptors, leads to alterations in feeding behavior in animals and may result in body-weight changes. However, the long-term effects of H3 receptors on anorexigenic activities for body-weight homeostasis have not been documented because of the off-target activity (31) and toxicity profile of H3 inhibitors (32). To define the roles of H3 receptors, we generated H3 receptor homozygous knockout mice by homologous recombination. Mice with disrupted H3 receptors demonstrated an obese phenotype that was characterized by increased body weight, food intake, and adiposity and by reduced energy expenditure.

Methods

Targeted gene disruption and in vivo experimental procedures. We isolated murine H3 receptor genomic clones from a 129Sv/J mouse genomic library (Stratagene, La Jolla, California, USA). The targeting vector contained a PGK-neomycin resistance cassette (neo), which replaced a 994-bp XbaI/SmaI genomic fragment that included exon 1. The RW4 embryonic stem (ES) cell line was transfected with a linearized vector by electroporation, and we obtained four homologous recombinants for the screened 576 G418-resistant clones. One of these clones was injected into C57BL/6N blastocysts. Embryos were transferred into the uterus of a 2.5-day pseudopregnant female mouse. Resultant chimeric mice were bred with C57BL/6N mice, and heterozygous mutants were bred for four generation with wild-type C57BL/6N mice. All experiments were carried out with littermates of heterozygous crosses of the fourth generation. Mice were maintained under conditions of controlled temperature (23°C ± 2°C) and light (7:00–19:00). Water and food (CA-1, CLEA Japan, Tokyo, Japan) were available ad libitum unless otherwise noted. The core body temperature of 26- to 43-week-old female mice (n = 9 or 10) was measured with a rectal thermometer (Physitemp Instruments, Clifton, New Jersey, USA). For body-weight measurements, mice were individually caged after weaning at 4 weeks of age, and weight was measured by a Libror balance (Shimadzu, Tokyo, Japan) every week. For 24-hour food-intake measurements, consumption of standard mouse chow CA-1 was measured every day for 1 week in 21- to 26-week-old male mice and 19- to 21-week-old female mice (n = 7–9). All values are given as means ± SEM. Statistics were performed with a two-tailed unpaired Student's t test (StatView, SAS Institute, Cary, North Carolina, USA). All animal procedures complied with NIH guidelines and were approved by the Banyu Animal Care and Usage Committee.

Southern blot genotyping analysis. We used 865-bp and 965-bp fragments located outside of the targeting vector on the 5′ and 3′ side as probes to screen for correctly targeted ES cell clones and subsequent mutant mice. Targeted disruption of the H3 receptor coding sequence with the PGK-neo resistance cassette introduced an additional BamHI site. Consequently, 5′ and 3′ probes detected BamHI fragments of approximately12 kb and 8.5 kb, respectively, from ES cells containing the targeted H3 receptor allele.

Binding experiments. Freshly dissected mouse brain (or hypothalamic section) was disrupted with a Polytron in 10 vol of homogenate buffer (20% sucrose, 154 mM NaCl, 10 mM KCl, 0.8 mM $CaCl_2$, 10 mM 3-[N-morpholino]-propanesulfonic acid [pH 7.4]). Debris was sedimented by 15 minutes of centrifugation at 1,000 *g*, after which membranes were sedimented at 90,000 *g* for 1 hour. Membranes were resuspended and washed twice with 5 mM HEPES/Tris buffer and frozen at –80°C. Tissue (0.2 mg of protein) was incubated for 40 minutes in 0.5 ml of 50 mM Tris-HCl at 30°C with 0.5 nM [^{3}H]N-α-methylhistamine (NAMHA) with or without cold NAMHA and then filtered over 0.3% polyethylenimine-presoaked Whatman GF/C filters (Whatman, Maidstone, United Kingdom). Filters were washed four times with 1 ml of 50 mM Tris-HCl. The radioactivity of the filters was determined by liquid scintillation counting. [^{3}H]NAMHA (specific activity, 82 Ci/mmol; PerkinElmer, Wellesley, Massachusetts, USA) concentration was 0.5 nM (50,000 degradation per minute [dpm]). [^{3}H]pyrilamine (specific activity, 20 Ci/mmol; PerkinElmer) concentration was 10 nM (130,000 dpm), and nonspecific binding was determined in the presence of 10 μM triprolidine (Tocris Cookson, Ellisville, Missouri, USA). Protein was assayed with a bicinchoninic acid reagent (Pierce, Cheshire, United Kingdom). Data analysis was performed using the GraphPad Prism data analysis software package and curve-fitting program (GraphPad Software, San Diego, California, USA). Data are representative of three experiments.

Body-composition analysis. Fat mass and lean body mass were measured as previously described (33); 20- to 25-week-old male and 16- to 17-week-old female mice (n = 3 or 4) were used.

Analysis of H1, H2, and H3 expression. Northern blot analysis was performed using 4 μg of brain total RNA for H3 and 4 μg of brain mRNA for H1 and H2 hybridizations. The hybridization probe consisted of mouse H3 cDNA (positions 432–1116), human H1 cDNA (positions 190–977), human H2 cDNA (positions 231–1026), and human GAPDH (positions 586–1037).

Analysis of UCP1, UCP2, and UCP3 expression. Total RNA was isolated from brown adipose tissue (BAT), white adipose tissue (WAT), and skeletal muscle. Five micrograms of total RNA was analyzed by Northern blotting. The hybridization probes consisted of mouse UCP1 cDNA (positions 745–1005), mouse UCP2 cDNA (positions 870–1177), and mouse UCP3 cDNA

(positions 212–542). Densitometry measurements were performed by FUJIX BAS2000 (Fuji-film, Tokyo, Japan) and normalized by GAPDH.

Measurement of locomotor activity. We evaluated locomotor activity of individually housed 16- to 21-week-old female mice (n = 9–11) with a cage rack (15 × 25 × 12 cm) photobeam system (Neuroscience, Tokyo, Japan). All the measurements were taken for 4 days in each group. The measurements taken on the last 3 days were used for data analysis.

Leptin sensitivity, energy expenditure, and indirect calorimetry. Leptin (3 mg/kg) was injected intraperitoneally into 11- to 16-week-old female mice on an ad libitum feeding schedule (n = 7) 1 hour before the dark cycle. Injection was performed on 3 consecutive days, and 24-hour food intake was measured after the third day of leptin injection. For the energy expenditure study, 20- to 27-week-old male mice (n = 10) were fasted for 21 hours (22:00–19:00), and feeding was initiated at the start of the dark cycle (19:00–22:00). During the feeding phase, water and food (MHF diet, CLEA) was available ad libitum. Body weight and 3-hour food intake were measured every day. We measured oxygen consumption using a open-circuit Oxymax system (Columbus Instruments, Columbus, Ohio, USA). We maintained 16- to 17-week-old female mice (n = 3 or 4) in a 12-hour light/dark cycle with food and water available ad libitum. Mice were maintained individually in specially built Plexiglas cages (20 × 10.5 × 12 cm), through which room air was passed at a rate of 0.75 l/min. We sequentially passed sample air through an oxygen analyzer (Columbus Instruments). Basal oxygen consumption was calculated as the average oxygen consumption during the light period (12:30–15:30), and total oxygen consumption was calculated as the 24-hour average. After the oxygen-consumption measurements, mice were sacrificed and lean body mass was determined as previously described (33); subsequently, each oxygen-consumption measurement was normalized to lean body mass.

Blood analysis. For the glucose tolerance tests, 26- to 28-week-old female mice (n = 4–6) were fasted for 14 hours and given glucose (2 g/kg) through intraperitoneal injection. For the insulin tolerance test, human insulin (0.75 U/kg; Novo Nordisk, Bagsværd, Denmark) was administered intraperitoneally to 26- to 28-week-old female mice (n = 4–6) that had been fasted for 3 hours. Blood was withdrawn from the tail at indicated times. Blood glucose levels were measured by AntsenseII (Daikin, Osaka, Japan). Plasma leptin and insulin levels were measured by ELISA (Morinaga, Yokohama, Japan). Commercial radioimmunoassay kits were used to measure plasma free T4 levels (Dainabot, Tokyo, Japan). Colorimetric assays were used for measurements of cholesterol, triacyl glycerol (TG; KYOWA, Tokyo, Japan), and FFAs (Wako, Tokyo, Japan). The ages of the animals when tested were as follows (for male and female mice, respectively): for leptin, insulin, and T4, 11–18 and 13–16 weeks; for FFA and cholesterol, 11–20 and 13–16 weeks; for TG, 14–19 and 17–24 weeks; and for glucose, 8–12 and 13–16 weeks.

Measurements of histamine/tele-methylhistamine. The mice were decapitated without pargyline injection, and their brains were quickly removed, placed on ice, and divided into five regions: forebrain (including the cortex and striatum), hippocampus, hypothalamus/thalamus, brainstem, and cerebellum. The brain samples were weighed and homogenized in 10 vol of 0.2 N perchloric acid with a sonicator. The homogenate was centrifuged at 10,000 *g* for 5 minutes at 4°C. The supernatant was neutralized (to pH 7–8) with 1 M borate buffer (pH 9.25). Female mice 20–26 weeks of age (n = 3) were used. We measured histamine by ELISA (Immunotech, Marseille, France) and *tele*-methylhistamine by RIA (Pharmacia Diagnostics, Uppsala, Sweden).

Intracerebroventricular administration of thioperamide and leptin. Drugs were injected into the right lateral cerebroventricle (0.5 mm posterior, 1.0 mm lateral, and 3.0 mm ventral to bregma) as previously described (34). Thioperamide (Tocris Cookson), neuropeptide Y (NPY; Peptide Institute, Osaka, Japan), and leptin (Genzyme Techne, Minneapolis, Minnesota, USA) were freshly dissolved in saline and infused at doses of 100 nmol, 2 μg, and 0.5 μg per mouse, respectively. Food intake was measured for 2 hours (thioperamide and NPY) and 24 hours (leptin) after infusion. The intracerebroventricular infusion volume of reagents was limited to a total volume of 5.0 μl. Mice used for these experiments were 20- to 30-week-old male mice (n = 9) for thioperamide and NPY and 18- to 34-week-old male mice (n = 5) for leptin.

Intraperitoneal administration of thioperamide. Thioperamide (10 mg/kg) and pargyline (65 mg/kg; Sigma-Aldrich, St. Louis, Missouri, USA) were injected intraperitoneally to female mice (37–54 weeks of age, n = 4) on an ad libitum feeding schedule. Their brains were quickly removed 90 minutes after the injection. The whole brains were used for *tele*-methylhistamine assay.

Results

H3 receptor gene disruption. Using a targeting vector that included the first exon of the H3 gene and homologous recombination, the coding region of the H3 receptor was replaced with a neomycin resistance cassette in ES cells. This targeting event resulted in deletion of an initiation Met codon and about 20% of the coding region, which included two transmembrane-spanning regions of the G protein–coupled H3 receptor. Southern blotting analysis of ES cells revealed that the neomycin gene was inserted within the H3 gene, which was indicated by a predicted change in the restriction enzyme map (Figure 1a). Targeted $H3^{+/-}$ ES cells were injected into blastocysts that produced chimeric mice and heterozygous $H3^{+/-}$ offspring. Southern blotting analysis confirmed that $H3^{+/-}$ mice were bred to create $H3^{-/-}$ mice (Figure 1b), and the mice were born at the expected mendelian frequencies ($H3^{+/+}$, 119 [28.9%]; $H3^{+/-}$, 200 [48.7%]; $H3^{-/-}$, 92 (22.4%); total, 411 mice). $H3^{-/-}$

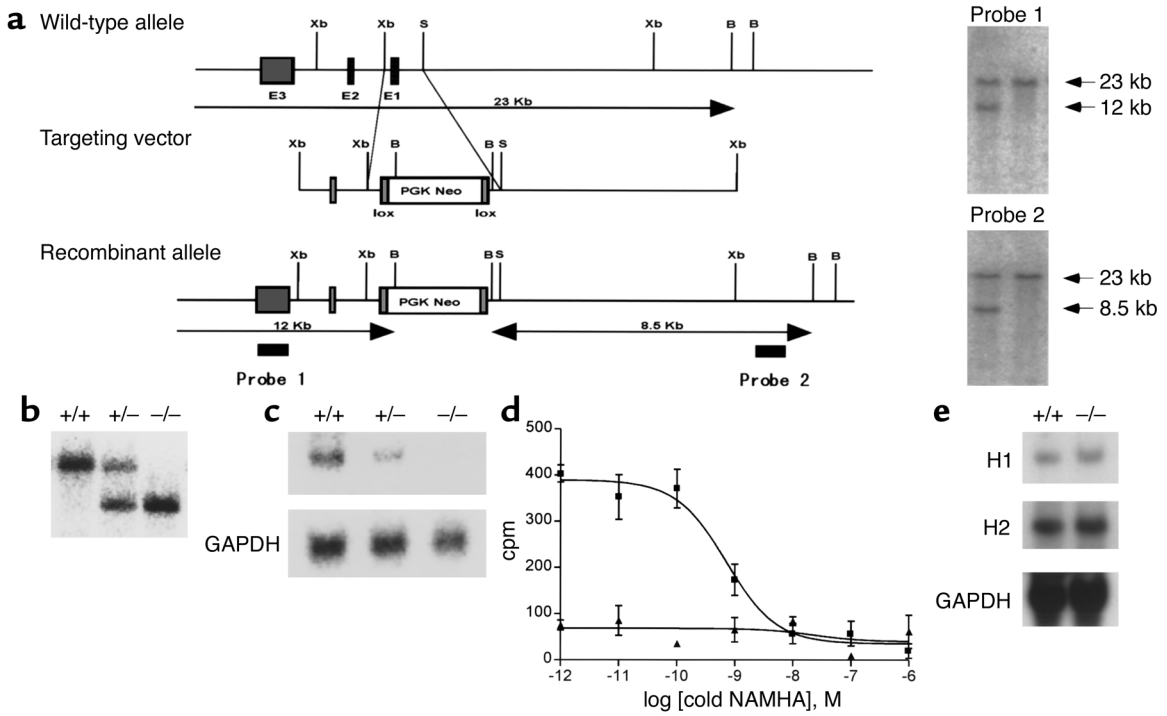

Figure 1

(**a**) Targeted disruption of the *H3* allele in mice. The mouse *H3* gene, targeting construct, and expected targeted allele are shown. Each of the three exons is indicated by black boxes. Horizontal arrows show the size of the expected fragments after BamHI digestion. Two probes that were used in Southern blot analysis are shown. B, BamHI; S, SmaI; Xb, XbaI. (**b**) Southern blot analysis of genomic DNA from mouse tail and hybridization after digestion of DNA with BamHI using probe 1 from (**a**). +/+, $H3^{+/+}$; +/–, $H3^{+/-}$; –/–, $H3^{-/-}$. (**c**) Northern blot analysis of brain total RNA. The H3 exon 3 probe was used in this experiment, and GAPDH was used as an internal control. (**d**) Agonist binding assay of brain membranes with [^{3}H]NAMHA. Data are representative of three experiments. $H3^{+/+}$ mice are indicated by squares and $H3^{-/-}$ mice by triangles. (**e**) Northern blot analysis of brain mRNA. H1- and H2-specific probes were used, and GAPDH served as an internal control.

and $H3^{+/-}$ mice were viable and fertile, and gross examination of the brain and other organs revealed that $H3^{-/-}$ mice did not have any overt abnormalities. Heterozygous H3 knockout mice were backcrossed into the C57BL/6 background for four generations.

Northern blotting analysis of brain total RNA from $H3^{-/-}$ mice did not display a detectable H3 mRNA signal, and H3 mRNA levels in $H3^{+/-}$ mice were less than those in $H3^{+/+}$ mice (Figure 1c). Binding studies with the H3 selective agonist NAMHA confirmed the absence of functional H3 receptors in brain membrane fractions and demonstrated that the brains of $H3^{-/-}$ mice lacked functional H3 receptors (Figure 1d). To exclude the possibility of developmental compensatory changes in the expression of other histamine receptors, the abundance of H1 and H2 mRNA in the brain was determined by Northern blotting analysis (Figure 1e). Levels of H1 and H2 mRNA in the $H3^{-/-}$ mice were similar to those in $H3^{+/+}$ littermates.

Physiological parameters of $H3^{-/-}$ mice and $H3^{+/+}$ littermates. To determine the importance of the H3 receptor in feeding regulation, the body weight of $H3^{-/-}$ mice was measured until the mice were 48 weeks old. $H3^{-/-}$ mutant mice had similar or slightly higher body weights than $H3^{+/+}$ littermates at 4 weeks, and they gained significantly more weight when compared with $H3^{+/+}$ or $H3^{+/-}$ littermates (Figure 2, a and b). Increased body weight was observed in both male and female $H3^{-/-}$ mice, and body-weight changes were observed in all of the $H3^{-/-}$ mice that were generated throughout this study. Body size did not differ significantly between $H3^{-/-}$ and $H3^{+/+}$ male mice when they were 16–18 weeks old (n = 10; length from nose to anus, 9.84 ± 0.13 cm in $H3^{-/-}$ mice and 9.73 ± 0.15 cm in $H3^{+/+}$ mice). At 40 weeks of age, $H3^{-/-}$ mice were 20.6% heavier than $H3^{+/+}$ littermate male mice and 13.2% heavier than $H3^{+/-}$ mice (20.8% and 4.7% for $H3^{+/+}$ female and $H3^{+/-}$ female mice, respectively). With respect to body composition, $H3^{-/-}$ mice showed greater fat deposition in ovarian (epididymal), mesenteric, retroperitoneal WAT, and BAT than did $H3^{+/+}$ mice and $H3^{+/-}$ mice. Also, fat mass in $H3^{-/-}$ mice was increased, whereas lean body mass in $H3^{-/-}$ mice was decreased (Table 1). This was consistent with the obese phenotype of $H3^{-/-}$ mice. Brain weight was not different among $H3^{-/-}$, $H3^{+/-}$, and $H3^{+/+}$ mice (data not shown).

Food intake and energy expenditure. We observed a modest but significant increase in daily food intake in mice that lacked the H3 receptor (Figure 2c). Simultaneous measurements of body weight and daily food intake revealed that body-weight gain correlated with food intake (Figure 2d). To measure energy expenditure, we determined spontaneous locomotor activity, oxygen consumption, and energy efficiency after food deprivation.

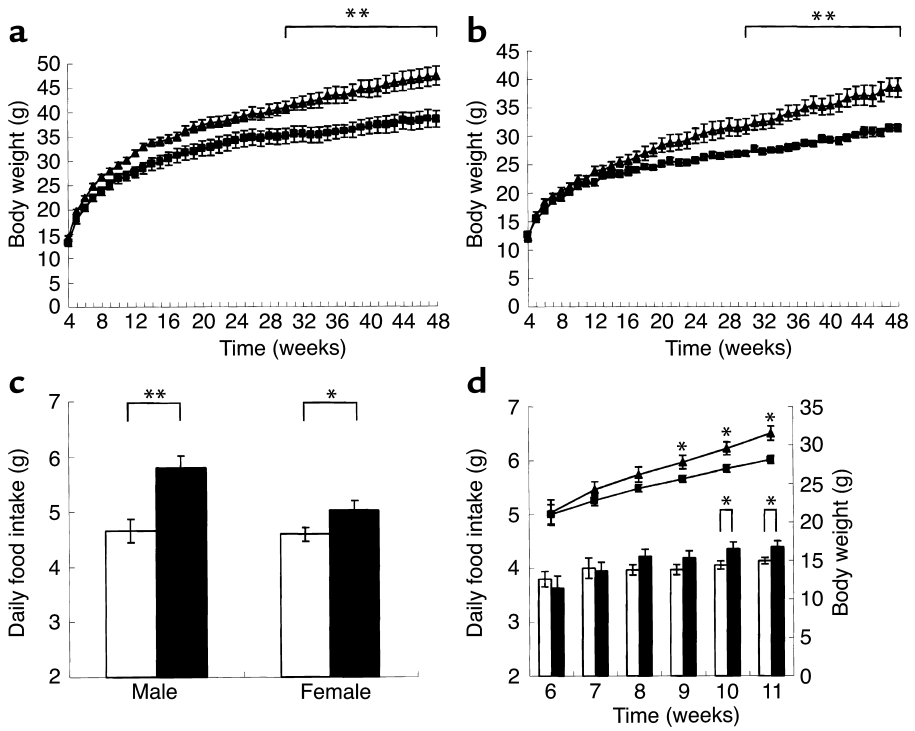

Figure 2
(**a**) Growth curve of $H3^{+/+}$ and $H3^{-/-}$ male mice (n = 9 or 10, $^{**}P < 0.01$). $H3^{+/+}$ mice are indicated by squares and $H3^{-/-}$ mice by triangles. (**b**) Growth curve of $H3^{+/+}$ and $H3^{-/-}$ female mice (n = 7 or 8, $^{**}P < 0.01$). $H3^{+/+}$ mice are indicated by squares and $H3^{-/-}$ mice by triangles. (**c**) Food intake of $H3^{+/+}$ and $H3^{-/-}$ mice. Shown is the 24-hour food consumption of 21- to 26-week-old male and 19- to 21-week-old female mice fed ad libitum (n = 7–9, $^{*}P < 0.05$, $^{**}P < 0.01$). $H3^{+/+}$ mice are indicated by white bars and $H3^{-/-}$ mice by black bars. (**d**) Growth curve and daily food intake of $H3^{+/+}$ and $H3^{-/-}$ male mice (n = 12–16, $^{*}P < 0.05$). $H3^{+/+}$ mice are indicated by squares and white bars and $H3^{-/-}$ mice by triangles and black bars.

In the latter experiment, we monitored body-weight changes in the mice after caloric intake was limited for 21 hours and after food intake was restricted to a short, 3-hour period each day (35, 36). In this experimental setup, $H3^{-/-}$ and $H3^{+/+}$ mice consumed similar amounts of food, which was about 5% of their body weight, during each 3-hour feeding period. However, body weight was reduced more prominently in $H3^{+/+}$ mice than in $H3^{-/-}$ mice (Figure 3a). This indicated that energy expenditure was decreased in $H3^{-/-}$ mice under this condition. To further investigate energy expenditure, oxygen consumption during resting and active phases was monitored. Under ad libitum feeding conditions, basal and total oxygen consumptions were reduced in $H3^{-/-}$ mice when compared with those in wild-type littermate controls (Figure 3b). The decrease in energy expenditure may be partially explained by changes that occurred in the locomotor activity of the $H3^{-/-}$ mice. Both total locomotor and dark-phase locomotor activity were significantly reduced in $H3^{-/-}$ mice when compared with those in $H3^{+/+}$ littermate controls (Figure 3, c and d). When measured by photobeam break, exploratory behavior in new environments and circadian rhythms of $H3^{-/-}$ mice were not significantly different from those of $H3^{+/+}$ mice (data not shown).

Glucose, insulin, and leptin sensitivity. We measured several plasma parameters that could further explain the obese phenotype of $H3^{-/-}$ mice. Data revealed that plasma leptin and insulin levels were significantly elevated in obese $H3^{-/-}$ mice, whereas plasma glucose, T4, FFA, cholesterol, and TG levels were not affected (Table 2). Fasting glycemia at 26–28 weeks of age was similar in $H3^{-/-}$ and $H3^{+/+}$ mice (0-minute time point in Figure 4b). To determine the extent of insulin resistance in $H3^{-/-}$ mice, insulin and glucose tolerance tests were performed. After intraperitoneal injection of insulin into mice that had fasted for 3 hours, $H3^{-/-}$ mice demonstrated reduced glucose clearance (Figure 4a). This observation was confirmed by a glucose tolerance test, in which $H3^{-/-}$ mice exhibited slow plasma clearance of intraperitoneally injected glucose (Figure 4b). Also, the response to leptin

Table 1
Body composition

Male	+/+ (n = 4)	+/– (n = 4)	–/– (n = 3)
Epididymal (g)	0.73 ± 0.15	0.90 ± 0.22	1.68 ± 0.26^{A}
Mesenteric (g)	0.32 ± 0.05	0.40 ± 0.09	$1.13 \pm 0.30^{A,B}$
Retroperitoneal (g)	0.43 ± 0.10	0.49 ± 0.12	$1.13 \pm 0.20^{A,B}$
BAT (g)	0.14 ± 0.01	0.13 ± 0.03	$0.27 \pm 0.02^{B,C}$
Fat mass (%)	17.15 ± 2.04	17.48 ± 3.54	27.62 ± 3.90^{A}
Lean body mass (%)	24.32 ± 0.64	24.26 ± 1.02	$19.96 \pm 1.07^{A,B}$
Female	**+/+ (n = 4)**	**+/– (n = 4)**	**–/– (n = 3)**
Ovarian (g)	0.45 ± 0.07	0.48 ± 0.04	$1.29 \pm 0.02^{C,D}$
Mesenteric (g)	0.14 ± 0.04	0.16 ± 0.03	$0.35 \pm 0.02^{C,D}$
Retroperitoneal (g)	0.17 ± 0.04	0.19 ± 0.03	$0.46 \pm 0.04^{C,D}$
BAT (g)	0.07 ± 0.01	0.08 ± 0.00	0.09 ± 0.01
Fat mass (%)	14.23 ± 0.94	12.95 ± 0.79	$28.43 \pm 2.14^{C,D}$
Lean body mass (%)	24.76 ± 0.18	24.68 ± 0.47	23.96 ± 0.13^{A}

Body composition of 20- to 25-week-old male and 16- to 17-week-old female mice. All values are means ± SEM. $^{A}P < 0.05$ versus +/+. $^{B}P < 0.05$ versus +/–. $^{C}P < 0.01$ versus +/+. $^{D}P < 0.01$ versus +/–.

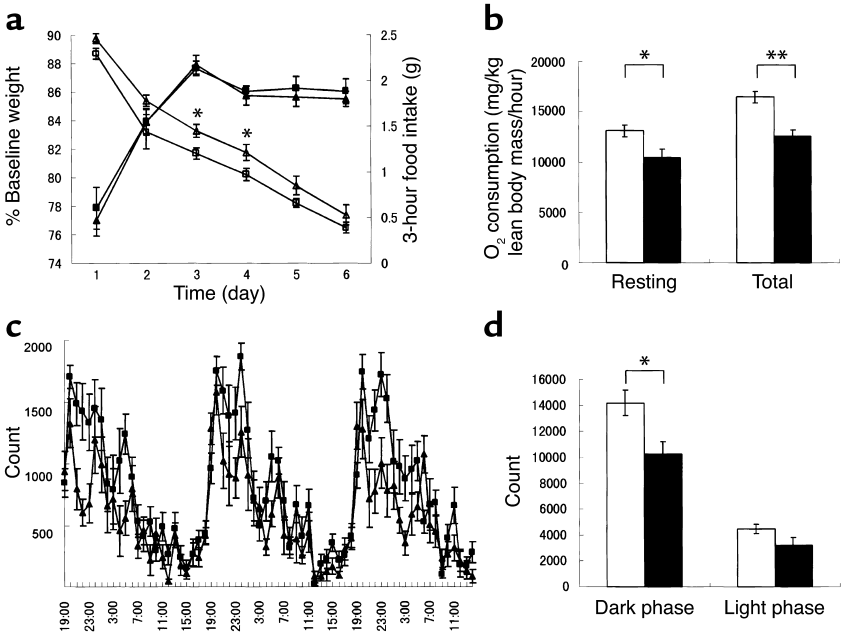

Figure 3
Caloric efficiency and locomotor activity of $H3^{+/+}$ and $H3^{-/-}$ mice. (**a**) Body weight and 3-hour food intake were measured after 21 hours of food restriction in 20- to 27-week-old male mice. $H3^{+/+}$ mice are indicated by filled squares (food intake) and open squares (body weight) and $H3^{-/-}$ mice by filled triangles (food intake) and open triangles (body weight) ($n = 10$, $^*P < 0.05$). (**b**) Basal and total oxygen consumption rate in 16- to 17-week-old female mice. Data are normalized to lean body mass. $H3^{+/+}$ mice are indicated by white bars and $H3^{-/-}$ mice by black bars ($n = 3$ or 4, $^*P < 0.05$; $^{**}P < 0.01$). (**c**) Light-phase and dark-phase locomotor activity in 16- to 21-week-old female mice. $H3^{+/+}$ mice are indicated by squares and $H3^{-/-}$ mice by triangles ($n = 9$–11). Measurements were taken for 4 consecutive days, and data from the last 3 days are shown. (**d**) Light-phase and dark-phase total locomotor activity in 16- to 21-week-old female mice. $H3^{+/+}$ mice are indicated by white bars and $H3^{-/-}$ mice by black bars ($n = 9$–11, $^*P < 0.05$). Measurements are averages for the last 3 days.

was reduced in $H3^{-/-}$ mice (Figure 4c), which was demonstrated by decreased sensitivity to the anorexigenic effects of leptin in H3 knockout mice as compared with that in littermate H3 wild-type controls.

Neuronal histamine and its metabolite concentrations. H3 receptors act as autoreceptors for histamine, and after the release from the terminus, histamine is converted to inactive *tele*-methylhistamine by histamine N-methyltransferase (HMT). To analyze the effects of H3 receptor depletion on neuronal histamine metabolism, brains of $H3^{-/-}$ and $H3^{+/+}$ mice were dissected, and total histamine and *tele*-methylhistamine concentrations were measured in each section (Table 3). We observed that there were changes in *tele*-methylhistamine concentrations in all regions of the brain in H3-disrupted mice. Increased concentrations of *tele*-methylhistamine indicated that the release and turnover of histamine is altered in H3 knockout mice. In comparison with other parts of brain, the hypothalamic/thalamic region had more dramatic changes in *tele*-methylhistamine concentrations, which were increased 2.3-fold as compared with concentrations in wild-type controls. In the hypothalamic/thalamic section, total histamine levels were also lower in $H3^{-/-}$ mice than in $H3^{+/+}$ littermates. Histamine concentrations in other parts of the brain and in the whole brain were not significantly different between $H3^{-/-}$ mice and $H3^{+/+}$ littermates (data not shown).

Metabolic marker changes in $H3^{-/-}$ mice. To investigate the metabolic changes in the $H3^{-/-}$ mice in more detail, the expression of several genes that are associated with food consumption and energy expenditure were measured by Northern blotting analysis (Figure 5a). In obese $H3^{-/-}$ mice, expression of *UCP1* and *UCP3* in BAT, *UCP3* in WAT, and *UCP3* in skeletal muscle was reduced. Densitometry measurements taken from Northern blotting indicated UCP1 mRNA in BAT, UCP3 mRNA in BAT, UCP3 mRNA in WAT, and UCP3 mRNA in skeletal muscle were reduced by 78%, 77%, 52%, and 64%, respectively, in $H3^{-/-}$ mice as compared with $H3^{+/+}$ control mice. Core body temperature decreased slightly but constantly in $H3^{-/-}$ mice ($n = 9$ or 10; 37.1 °C ± 0.1 °C in $H3^{-/-}$ mice and 37.5 °C ± 0.1 °C in $H3^{+/+}$ mice in the dark phase). These changes provide a possible mechanistic explanation for the decreases in energy expenditure and the increases in body weight that are observed in

Table 2
Plasma hormone and metabolite levels

Male	+/+ (n = 6–12)	+/– (n = 6–11)	–/– (n = 5–9)
Leptin (ng/ml)	3.4 ± 0.7	5.5 ± 0.9	7.2 ± 1.3[A]
Glucose (mg/dl)	151.0 ± 10.8	161.9 ± 8.8	157.0 ± 4.7
Insulin (ng/ml)	1.30 ± 0.16	1.91 ± 0.47	2.30 ± 0.32[A]
T4 (μg/ml)	5.07 ± 0.46	4.89 ± 0.33	5.62 ± 0.34
FFAs (mmol/l)	0.76 ± 0.10	0.79 ± 0.08	0.69 ± 0.09
Cholesterol (mg/dl)	83.2 ± 3.7	86.4 ± 6.0	93.8 ± 5.1
TG (mg/dl)	88.6 ± 13.7	86.4 ± 7.6	67.3 ± 16.6
Female	**+/+ (n = 7–9)**	**+/– (n = 6–9)**	**–/– (n = 6–7)**
Leptin (ng/ml)	2.5 ± 0.3	2.7 ± 0.4	11.2 ± 2.6[B,C]
Glucose (mg/dl)	146.5 ± 6.1	145.6 ± 6.3	149.8 ± 6.3
Insulin (ng/ml)	0.46 ± 0.05	0.45 ± 0.08	1.22 ± 0.19[B,C]
T4 (μg/ml)	4.75 ± 0.24	4.43 ± 0.35	4.29 ± 0.28
FFAs (mmol/l)	0.75 ± 0.05	0.71 ± 0.05	0.78 ± 0.08
Cholesterol (mg/dl)	69.4 ± 2.5	78.0 ± 4.0	76.2 ± 5.6
TG (mg/dl)	62.1 ± 4.3	55.2 ± 6.5	50.2 ± 3.9

Blood from freely fed mice was used. All values are means ± SEM. The ages of the animals are as follows (for male and female mice, respectively): for leptin, insulin, and T4, 11–18 and 13–16 weeks; for FFA and cholesterol, 11–20 and 13–16 weeks; for TG, 14–19 and 17–24 weeks; and for glucose, 8–12 and 13–16 weeks. [A]$P < 0.05$ versus +/+. [B]$P < 0.01$ versus +/+. [C]$P < 0.01$ versus +/–.

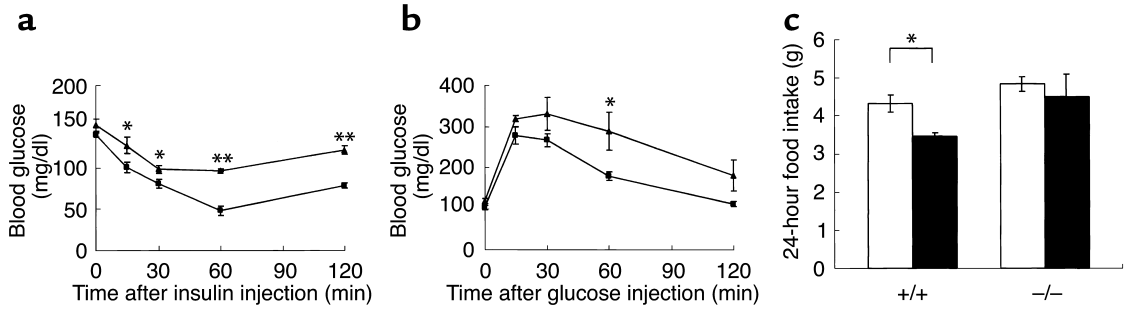

Figure 4
Insulin and glucose tolerance test for H3$^{+/+}$ mice (squares) and H3$^{-/-}$ mice (triangles). (**a**) Insulin tolerance test. Insulin was injected intraperitoneally into 26- to 28-week-old, 3-hour fasted female mice. Blood glucose levels were determined at the indicated times (n = 4–6, *P < 0.05; **P < 0.01). (**b**) Glucose tolerance test. Glucose was injected intraperitoneally into 26- to 28-week-old, 14-hour fasted female mice. Blood glucose levels were determined at the indicated times (n = 4–6, *P < 0.05). (**c**) Leptin sensitivity test. Leptin was injected intracerebroventricularly into 18- to 34-week-old male mice, and 24-hour food intake was determined (n = 5, *P < 0.05). White bars indicate saline and black bars leptin.

homozygous H3$^{-/-}$ mice. Expression of the orexigenic peptides NPY (37) and melanin-concentrating hormone (MCH) (38) did not change (data not shown).

Anorexigenic activity of thioperamide in H3$^{-/-}$ mice. The modulation of histamine has been shown to change feeding behaviors in mammals, and histaminergic modification is reported to be regulated by the H3 receptor. To confirm the role of the H3 receptor in feeding behavior directly, we tested the anorexigenic effect of thioperamide in NPY-induced food intake in H3$^{-/-}$ mice and H3$^{+/+}$ littermates. The H3 antagonist thioperamide was administered intracerebroventricularly with NPY, and acute food intake during a 2-hour period was monitored. As a result, the hyperphagic response to NPY was similar between H3$^{-/-}$ and H3$^{+/+}$ littermates; however, the anorexigenic activity of thioperamide was not observed in H3$^{-/-}$ mice (Figure 5b). Moreover, release of histamine on intraperitoneal injection of thioperamide was totally abolished in H3$^{-/-}$ mice (n = 4; *tele*-methylhistamine concentration measured in whole brain: H3$^{+/+}$, 301 ± 15 ng/g brain weight [saline] and 543 ± 62 ng/g brain weight [thioperamide]; H3$^{-/-}$, 751 ± 52 ng/g brain weight [saline] and 633 ± 53 ng/g brain weight [thioperamide]).

Discussion

The data presented here indicate that H3 receptors are involved in mediation of body-weight regulation and modulation of food intake and energy expenditure in mice. Possible mechanisms are autoregulation of histaminergic neurons and inhibition of histamine release or heterologous presynaptic effects on, for example, serotonergic neurons. The biosynthesis and release of histamine is regulated through H3 receptors, which are on presynaptic membranes. H3 receptor agonists, such as histamine, inhibit this process, whereas H3 receptor antagonists promote the release of histamine. The modulation of histaminergic tone in the CNS has been implicated in several behavioral changes, including food and water intake. Our results confirm that H3 autoregulatory mechanisms are important for body-weight homeostasis. However, the involvement of other neuronal systems in feeding regulation, especially serotonergic systems, cannot be addressed in this study. H3 receptors are known to localize on the other monoaminergic terminals and to function as heteroreceptors.

Consistent with an increased body weight, we observed an increased fat mass in H3$^{-/-}$ mice. H3$^{-/-}$ mice had an increase in the weight of epididymal (ovarian for female), mesenteric, retroperitoneal WAT, and BAT when compared with H3$^{+/+}$ mice; these changes reflect an increase in fat mass in H3$^{-/-}$ mice. We also observed an H3 gene dose response in some phenotypes of H3$^{+/-}$ mice, which included effects on adipose weight and body weight. Increased fat mass in H3$^{-/-}$ mice correlated with an increase in plasma leptin

Table 3
Brain histamine and metabolite levels

	Forebrain	Hypothalamus/Thalamus	Hippocampus	Cerebellum	Brainstem
Histamine (ng/g tissue)					
+/+ (n = 3)	20.6 ± 0.7	33.9 ± 0.5	3.5 ± 0.9	2.2 ± 0.4	5.1 ± 1.7
–/– (n = 3)	19.4 ± 2.0	28.6 ± 1.3^{A}	2.1 ± 0.6	5.9 ± 3.5	5.4 ± 2.6
tele-methylhistamine (ng/g tissue)					
+/+ (n = 3)	134.8 ± 18.4	145.1 ± 8.3	83.2 ± 6.1	82.2 ± 0.3	97.2 ± 5.3
–/– (n = 3)	288.9 ± 21.4^{B}	340.0 ± 13.2^{B}	127.9 ± 14.5^{A}	101.2 ± 0.8^{B}	130.8 ± 8.8^{A}

Brain histamine and *tele*-methylhistamine were measured in 20- to 26-week-old female mice. All values are means ± SEM. ^{A}P < 0.05 versus +/+. ^{B}P < 0.01 versus +/+.

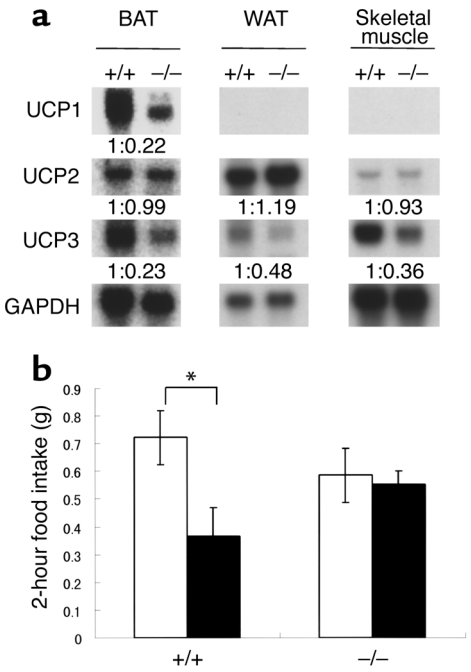

Figure 5

Metabolic marker changes and thioperamide activity. (**a**) Expression of UCP genes in BAT, WAT, and skeletal muscle total RNA. Specific probes for each UCP were used, and GAPDH served as an internal control. Densitometry measurements on each band are shown as wild-type littermate control normalized by GAPDH. +/+, $H3^{+/+}$ mice; –/–, $H3^{-/-}$ mice. (**b**) Thioperamide activity in $H3^{+/+}$ and $H3^{-/-}$ mice in NPY-induced feeding. Thioperamide was administered intracerebroventricularly into 20- to 30-week-old male mice. Food intake was measured at 2-hour intervals in mice under ad libitum feeding conditions ($n = 9$, $^*P < 0.05$). White bars indicate NPY/saline and black bars, NPY/thioperamide.

and insulin levels, because increases in adipose weight are known to cause increases in leptin and insulin secretion in rodents.

Changes in energy expenditure may be another important contributor to increased body weight in $H3^{-/-}$ mice. In experimental studies in which $H3^{+/+}$ and $H3^{-/-}$ mice consumed similar but limited amounts of food, $H3^{+/+}$ mice had more prominent reductions in body weight than did $H3^{-/-}$ mice. In addition, both basal and total oxygen consumption rates under ad libitum feeding conditions decreased in $H3^{-/-}$ mice. Reduction in energy expenditure could also be a reflection of the apparent decrease in locomotor activity in $H3^{-/-}$ mice; however, we have not observed any behavioral changes such as circadian rhythm alterations or narcolepsy-like phenotypes (39) in $H3^{-/-}$ mice. Similar changes in locomotor activities of H3 receptor–deficient mice have been reported recently (40). Moreover, the expression of genes associated with energy homeostasis, *UCP1* and *UCP3* (41), was changed. Changes in UCP expression may be caused by impaired leptin signaling in the hypothalamus of $H3^{-/-}$ mice, since leptin not only regulates appetite but also regulates UCP expression in peripheral tissues like BAT and WAT (42). It has been reported that injection of α-fluoromethylhistidine, an inhibitor of histamine synthesis, before leptin administration attenuated the anorexigenic action of leptin (24), and leptin receptor–deficient (*db/db*) mice and Zucker fatty (*fa/fa*) rats have decreased levels of hypothalamic histamine (23).

A possible mechanism underlying all these observations is impaired regulation of histaminergic neurons. The presence of increased levels of *tele*-methylhistamine, which is a metabolite of histamine, in all brain areas confirmed our hypothesis. We hypothesized that the lack of autoreceptors, which results in continuous release of histamine from presynaptic neurons in $H3^{-/-}$ mice, prevents the termination of histamine release that is normally caused by exposure to histamine. Continuous histamine release may overload histamine-synthesis machinery and lead to a chronic shortage of histamine in the nerve terminus. Reductions in the levels of neurotransmitters and changes in their turnover rates in the targeted disruption of autoreceptors in mice have been described previously in α_{2A}-adrenergic receptor knockout (43) and 5-HT_{1B} serotonergic autoreceptor knockout (44) mice.

Since several H3 antagonists have been shown to increase histamine release and suppress food intake (19–21, 26–30), increases in the concentration of *tele*-methylhistamine in the hypothalamic region of the brains of $H3^{-/-}$ mice coupled with increased food intake were unexpected. The relationship between increased brain *tele*-methylhistamine concentrations and increased food intake could be explained by the desensitization of histamine H1 receptors. Because of the chronic release of histamine, the function of the H1 receptors could be downregulated to compensate for the constitutive histamine exposure. We found that H1 receptors were slightly downregulated in the hypothalamic region of $H3^{-/-}$ mice when compared with those in $H3^{+/+}$ littermate controls ($n = 3$; 228 ± 53.9 cpm in $H3^{+/+}$ mice and 143 ± 30.9 cpm in $H3^{-/-}$ mice in [^{3}H]pyrilamine binding in hypothalamic membrane). These data could imply that the downregulation of H1 receptors may be partially responsible for increased food intake. However, more studies are needed to address the involvement of H1 receptors in histamine-mediated appetite regulation (45, 46).

Intracerebroventricular injection of thioperamide into $H3^{-/-}$ mice confirmed our hypothesis that H3 receptors regulate food intake through histamine modulation. The release of histamine was not observed in $H3^{-/-}$ mice after administration of thioperamide, indicating that thioperamide regulates histamine release through H3 receptors. Also, anorexigenic activities of thioperamide in NPY-induced hyperphagia were not detected in $H3^{-/-}$ mice; however, thioperamide attenuated NPY-induced hyperphagia in $H3^{+/+}$ littermates. These results imply that the anorexigenic activities of thioperamide are mediated through H3 receptors by modulation of brain histaminergic tone.

From the data presented, we infer that H3 inactivation in mice alters the regulation of body weight, energy expenditure, and food intake and leads to an obese hyperphagic mouse with reduced energy expenditure and insulin and leptin resistance. It is conceivable that pharmacological manipulation of the H3 receptor with selective compounds may be applied to the treatment of obesity in humans.

Acknowledgments

We thank M. Yoshida, L. Van der Ploeg, D. Marsh, A. Kanatani, and S. Tokita for support and comments on the project; J. Winward and K. Marcopul for editorial assistance; H. Ohta, M. Maetani, S. Okuda, R. Yoshimoto, and A. Ishihara for technical work; and members of the Functional Genomics group for their informative discussions.

1. Ring, J. 1985. Histamine and allergic diseases. In *New trends in allergy*. Springer-Verlag Press. Berlin, Germany. 44–77.
2. Zhang, M.Q., Leurs, R., and Timmerman, H. 1997. Histamine H1-receptor antagonists. In *Burger's medicinal chemistry and drug discovery*. 5th edition. M.E. Wolff, editor. John Wiley and Sons. New York, New York, USA. 495–559.
3. van der Goot, H., Bast, A., and Timmerman, H. 1991. Structural requirements for histamine H2 agonists and H2 antagonists. In *Handbook of experimental pharmacology*. B. Uvnas, editor. Springer-Verlag. Berlin, Germany. 573–749.
4. Schwartz, J.C., and Haas, H.L. 1992. *The histamine receptor*. Wiley Liss. New York, New York, USA.
5. Hill, S.J. 1990. Distribution, properties and functional characteristics of three classes of histamine receptor. *Pharmacol. Rev.* **42**:45–83.
6. Schwartz, J.C., Arrang, J.M., Garbarg, M., Pollard, H., and Ruat, M. 1991. Histaminergic transmission in the mammalian brain. *Physiol. Rev.* **71**:1–51.
7. Tohyama, M., and Takatsuji, K. 1998. *Atlas of neuroactive substances and their receptors in the rat*. Oxford University Press. Oxford, United Kingdom. pp. 54–63.
8. Leurs, R., Smit, M.J., and Timmerman, H. 1995. Molecular pharmacological aspects of histamine receptors. *Pharmacol. Ther.* **66**:413–463.
9. Lovenberg, T.W., et al. 1999. Cloning and functional expression of the human histamine H3 receptor. *Mol. Pharmacol.* **55**:1101–1107.
10. Oda, T., Morikawa, N., Saito, Y., Masuho, Y., and Matsumoto, S. 2000. Molecular cloning and characterization of a novel type of histamine receptor preferentially expressed in leukocytes. *J. Biol. Chem.* **275**:36781–36786.
11. Schlicker, E., Malinowska, B., Kathmann, M., and Gothert, M. 1994. Modulation of neurotransmitter release via histamine H3 heteroreceptors. *Fundam. Clin. Pharmacol.* **8**:128–137.
12. Lin, J.S., et al. 1990. Involvement of histaminergic neurons in arousal mechanisms demonstrated with H3-receptor ligands in the cat. *Brain Res.* **523**:325–330.
13. Clapham, J., and Kilpatrick, G.J. 1994. Thioperamide, the selective histamine H3 receptor antagonist, attenuates stimulant-induced locomotor activity in the mouse. *Eur. J. Phamacol.* **259**:107–114.
14. Imamura, M., Smith, N.C., Garbarg, M., and Levi, R. 1996. Histamine H3-receptor-mediated inhibition of calcitonin gene-related peptide release from cardiac C fibers. A regulatory negative-feedback loop. *Circ. Res.* **78**:863–869.
15. Lecklin, A., Etu-Seppala, P., Stark, H., and Tuomisto, L. 1998. Effects of intracerebroventricularly infused histamine and selective H1, H2, and H3 agonists on food and water intake and urine flow in Wistar rats. *Brain Res.* **793**:279–288.
16. Leurs, R., Blandina, P., Tedford, C., and Timmerman, H. 1998. Therapeutic potential of histamine H3 receptor agonists and antagonists. *Trends Pharmacol. Sci.* **19**:177–184.
17. Blandina, P., et al. 1996. Inhibition of cortical acetylcholine release and cognitive performance by histamine H3 receptor activation in rats. *Br. J. Pharmacol.* **119**:1656–1664.
18. Inoue, I., et al. 1996. Impaired locomotor activity and exploratory behavior in mice lacking histamine H1 receptors. *Proc. Natl. Acad. Sci. USA.* **93**:13316–13320.
19. Sakata, T., Yoshimatsu, H., and Kurokawa, M. 1997. Hypothalamic neuronal histamine: implications of its homeostatic control of energy metabolism. *Nutrition*. **13**:403–411.
20. Bjenning, C., Johannesson, U., Juul, A.G., Lange, K.Z., and Rimvall, K. 2000. Peripherally administered ciproxifan elevates hypothalamic histamine levels and potently reduces food intake in the Sprague Dawley rat. *Int. Sendai Histamine Symp.* P39–P40.
21. Sakata, T. 1995. Histamine receptor and its regulation of energy metabolism. *Obes. Res.* **3**(Suppl 4):S541–S548.
22. Tuomisto, L., Yamatodani, A., Jokkonen, J., Sainio, E.L., and Airaksinen, M.M. 1994. Inhibition of brain histamine synthesis increases food intake and attenuates vasopressin response to salt loading in rats. *Meth. Find. Exp. Clin. Pharmacol.* **16**:355–359.
23. Machidori, H., et al. 1992. Zucker obese rats: defect in brain histamine control of feeding. *Brain Res.* **590**:180–186.
24. Yoshimatsu, H., et al. 1999. Hypothalamic neuronal histamine as a target of leptin in feeding behavior. *Diabetes.* **48**:2286–2291.
25. Fukagawa, K., et al. 1989. Neuronal histamine modulates feeding behavior through H1 receptor in rat hypothalamus. *Am. J. Physiol.* **256**:R605–R611.
26. Lecklin, A., and Tuomisto, L. 1998. The blockade of H1 receptors attenuates the suppression of feeding and diuresis induced by inhibition of histamine catabolism. *Pharmacol. Biochem. Behav.* **59**:753–758.
27. Sakata, T., Ookuma, K., Fujimoto, K., Fukagawa, K., and Yoshimatsu, H. 1991. Histaminergic control of energy balance in rats. *Brain Res. Bull.* **27**:371–375.
28. Attoub, S., et al. 2001. The H3 receptor is involved in cholecystokinin inhibition of food intake in rats. *Life Sci.* **69**:469–478.
29. Doi, T., et al. 1994. Hypothalamic neuronal histamine regulates feeding circadian rhythm in rats. *Brain Res.* **641**:311–318.
30. Ookuma, K., et al. 1993. Neuronal histamine in the hypothalamus suppresses food intake in rats. *Brain Res.* **628**:235–242.
31. Leurs, R., et al. 1995. Evaluation of the receptor selectivity of the H3 receptor antagonists, iodophenpropit and thioperamide: an interaction with the 5-HT3 receptor revealed. *Br. J. Pharmacol.* **116**:2315–2321.
32. Onderwater, R.C., et al. 1998. Cytotoxicity of a series of mono- and di-substituted thiourea in freshly isolated rat hepatocytes: a preliminary structure-toxicity relationship study. *Toxicology*. **125**:117–129.
33. Cohen, P., et al. 2002. Role for stearoyl-CoA desaturase-1 in leptin-mediated weight loss. *Science*. **297**:240–243.
34. Masaki, T., Yoshimatsu, H., Chiba, S., Watanabe, T., and Sakata, T. 2001. Central infusion of histamine reduces fat accumulation and upregulates UCP family in leptin-resistant obese mice. *Diabetes*. **50**:376–384.
35. Kushi, A., et al. 1998. Obesity and mild hyperinsulinemia found in neuropeptide Y-Y1 receptor-deficient mice. *Proc. Natl. Acad. Sci. USA.* **95**:15659–15664.
36. Ohki-Hamazaki, H., et al. 1997. Mice lacking bombesin receptor subtype-3 develop metabolic defects and obesity. *Nature*. **390**:165–169.
37. Erickson, J.C., Hollopeter, G., and Palmiter, R.D. 1996. Attenuation of the obesity syndrome of *ob/ob* mice by the loss of neuropeptide Y. *Science*. **274**:1704–1707.
38. Shimada, M., Tritos, N.A., Lowell, B.B., Flier, J.S., and Maratos-Flier, E. 1998. Mice lacking melanin-concentrating hormone are hypophagic and lean. *Nature*. **396**:670–674.
39. Chemelli, R.M., et al. 1999. Narcolepsy in orexin knockout mice: molecular genetics of sleeping regulation. *Cell*. **98**:437–451.
40. Toyota, H., et al. 2002. Behavioral characterization of mice lacking histamine H3 receptors. *Mol. Pharmacol.* **62**:389–397.
41. Boss, O., Hagen, T., and Lowell, B.B. 2000. Uncoupling proteins 2 and 3: potential regulators of mitochondrial energy metabolism. *Diabetes*. **49**:143–156.
42. Cusin, I., et al. 1998. Chronic central leptin infusion enhances insulin-stimulated glucose metabolism and favors the expression of uncoupling proteins. *Diabetes*. **47**:1014–1019.
43. Altman, J.D., et al. 1999. Abnormal regulation of the sympathetic nervous system in α_{2A}-adrenergic receptor knockout mice. *Mol. Pharmacol.* **56**:154–161.
44. Ase, A.R., Reader, T.A., Hen, R., Riad, M., and Descarries, L. 2000. Altered serotonin and dopamine metabolism in the CNS of serotonin 5-HT_{1A} or 5-HT_{1B} receptor knockout mice. *J. Neurochem.* **75**:2415–2426.
45. Masaki, T., Yoshimatsu, H., Chiba, S., Watanabe, T., and Sakata, T. 2001. Targeted disruption of histamine H1-receptor attenuates regulatory effects of leptin on feeding, adiposity, and UCP family in mice. *Diabetes*. **50**:385–391.
46. Mollet, A., et al. 2001. Histamine H1 receptors mediate the anorectic action of the pancreatic hormone amylin. *Am. J. Physiol.* **281**:R1442–R1448.